First in situ temperature measurements in the summer mesosphere at very high latitudes (78°N)

Franz-Josef Lübken and Arno Müllemann
Leibniz-Institute of Atmospheric Physics, Kühlungsborn, Germany

Received 4 April 2002; revised 3 July 2002; accepted 12 July 2002; published 20 March 2003.

[1] A total of 24 temperature profiles from ~92 to 55 km were obtained from falling sphere flights in Longyearbyen (Svalbard, 78°N) from 16 July to 14 September 2001. The thermal structure of the upper mesosphere during the summer season (here from mid-July to 23 August) is characterized by very low temperatures and little variability. The mesopause temperature decreases slightly from ~130 K in mid-July to 126–128 K in late July/beginning of August. The mesopause altitude in summer is ~89 km. Compared to 10° further south (69°N, Andøya), the mesopause temperature is very similar in mid-July but is significantly colder by 6–8 K in the second half of July and in August. Part of this difference (especially in late August) is due to the later transition from summer to winter in Longyearbyen. The mesopause altitude is higher by approximately 1 km at Longyearbyen compared to Andøya. At 82 km, the temperature in summer is very close to 150 K, very similar to other Arctic and Antarctic stations (''equithermal submesopause''). The temperatures in the upper mesosphere are significantly lower compared to COSPAR International Reference Atmosphere (CIRA, 1986) by up to 20 K. Assuming model water vapor concentrations, we derived the degree of saturation of water vapor (S). In summer, there is an extended altitude range (82–92 km) with supersaturation (S > 1). Occasionally, very high supersaturation was derived (S > 100). Our temperature measurements are in general agreement with the occurrence morphology of polar mesosphere summer echoes (PMSE). However, double layered structures frequently observed in PMSEs are not a prominent feature of the temperatures in the upper mesosphere. *INDEX TERMS:* 0340 Atmospheric Composition and Structure: Middle atmosphere—composition and chemistry; 0350 Atmospheric Composition and Structure: Pressure, density, and temperature; 0399 Atmospheric Composition and Structure: General or miscellaneous; *KEYWORDS:* mesosphere, temperature, arctic, PMSE, transition, rockets

Citation: Lübken, F.-J., and A. Müllemann, First in situ temperature measurements in the summer mesosphere at very high latitudes (78°N), *J. Geophys. Res.*, *108*(D8), 8448, doi:10.1029/2002JD002414, 2003.

1. Introduction

[2] The thermal structure of the high latitude mesosphere and lower thermosphere (HLMLT) has stimulated many experimental and theoretical studies to improve our understanding of the physical and chemical processes leading to the peculiar seasonal variation of temperatures which are (generally speaking) ''high'' in winter and ''low'' in summer. From these studies it has become clear that only a complicated balance between various energy and momentum sources and sinks can lead to the observed thermal structure [e.g., *Garcia and Solomon*, 1985; *Berger and Von Zahn*, 1999; *Akmaev*, 2001; *Zhu et al.*, 2001]. The most important contributions to the energy budget are absorption of solar radiation, radiative cooling, adiabatic heating and cooling caused by vertical motions induced by ageostrophic winds, heating by deposition of turbulence energy, turbulent heat conduction, and heating by exothermic chemical reactions. The polar mesopause region has gained special interest in recent decades since it is a major challenge to reproduce the very low summer mesopause temperatures in models, and since some unique features in the terrestrial atmosphere occur only here, for example, noctilucent clouds (NLC), polar mesosphere summer echoes (PMSE), and polar mesosphere clouds (PMC). Since most of the contributions to the energy and momentum budget of the HLMLT region presumably depend on latitude and season, further insight in the energy and momentum budget can be gained from measurements at latitudes where practically no data are yet available (there have been Russian meteorological rocket launches at Heiss Island, 81°N, but this technique gives reliable temperatures below ~65 km only). In this paper, we report first measurements of the thermal structure in the summer mesosphere at very high latitudes (78°N).

[3] In section 2, we present details on the experimental technique, the measurements performed during the field

0148-0227/03/2002JD002414$09.00

campaign, and the experimental results. In section 3, we compare our results with measurements at lower latitudes (69°N) and with model predictions. We also discuss implications for the occurrence probability of small-scale layers (NLC, PMSE, and PMC) in the high latitude summer mesopause region. Finally, we summarize our findings in section 4.

2. Measurements

[4] From 16 July to 14 September 2001, a series of small meteorological rockets were launched from a mobile launcher installed close to Longyearbyen (78°15′N, 15°24′O) on the north polar island Spitsbergen which is part of the archipelago Svalbard. The campaign is part of the Rocket-borne Observations in the Middle Atmosphere (ROMA) project. The measurements reported here were performed employing the falling sphere (FS) technique. A small rocket transports a folded up sphere, made of metalized mylar, to an altitude of typically 110 km. After it is released the sphere inflates to 1 m diameter and falls through the atmosphere whereby it decelerates. A high-precision radar tracks the descent trajectory, which is then used in the equations of motion to determine atmospheric density and horizontal winds. Temperatures are obtained by integrating the density profile assuming hydrostatic equilibrium. Density and temperature retrieval starts at altitudes where the sphere significantly experiences deceleration, i.e., at approximately 95 km. The temperature at the top of the FS profile (''start temperature'' T_o) has to be taken from independent measurements or from a model. We have taken T_o from a preliminary data analysis of the potassium lidar measurements (described below) which gave smoothed and interpolated temperature profiles for the entire ROMA period (Höffner, private communication, 2002). The availability of lidar temperatures significantly improves the FS accuracy in the upper part of the profiles since it substantially reduces the uncertainty about the start temperature. The height-dependent sphere reaction time constant causes a smoothing of the density, temperature, and wind profiles. The smallest scales detectable are typically 8, 3, and 0.8 km at 85, 60, and 40 km, respectively [*Schmidlin*, 1991; *Lübken et al.*, 1994]. We note that the FS technique shows excellent overall agreement with entirely different rocket-borne temperature measurements with much better altitude resolution [*Rapp et al.*, 2001, 2002]. In particular, the mean mesopause structure, which corresponds to a spatial scale of ~10–15 km, is nicely reproduced. During some of the ROMA flights, we have observed a peculiar small-scale sinusoidal variation of unknown origin in the trajectory data of the lower part of the flight (below approximately 55 km). Since the reason for these variations is not yet understood and since we concentrate on the mesosphere in this paper, we decided to ignore the FS data below 55 km.

[5] In Table 1, the dates and times of all FS flights during the ROMA campaign are listed. For completeness we have included rocket flights where high resolution wind measurements with the foil cloud (''chaff'') technique were performed [*Widdel*, 1990]. As can be seen from this table, a time interval of 3–4 days between two FS flights was chosen to achieve a good temporal coverage of the seasonal variation of temperatures. Occasionally, two launches were performed on the same day to study special events, for example a NLC. Most of the launches took place close to local noon, i.e., at the same time of the day, to avoid tidal effects and to facilitate comparison with measurements at other latitudes (in particular at Andøya, 69°) where most of the measurements were also performed close to local noon or to midnight, i.e., at the same phase of the most prominent semidiurnal tide [*Forbes*, 1982].

Table 1. Meteorological Rocket Flights During the ROMA/Svalbard Campaign[a]

Flight Label	Date	Time (UT)
ROFS01	16 July 2001	1125:00
ROFS02	19 July 2001	1117:20
ROFS03	22 July 2001	1220:00
ROCH04	22 July 2001	1255:00
ROFS05	25 July 2001	1000:00
ROFS06	28 July 2001	1007:00
ROFS07	31 July 2001	0900:00
ROCH08	31 July 2001	0950:00
ROFS09	02 Aug. 2001	1800:00
ROFS10	06 Aug. 2001	0938:00
ROFS11	09 Aug. 2001	1013:00
ROFS12	12 Aug. 2001	1016:00
ROFS13	17 Aug. 2001	1136:00
ROCH14	17 Aug. 2001	1219:00
ROFS15	20 Aug. 2001	1025:00
ROFS16	20 Aug. 2001	1948:00
ROFS17	23 Aug. 2001	1009:00
ROFS18	27 Aug. 2001	1045:00
ROFS19	28 Aug. 2001	2148:39
ROCH20	28 Aug. 2001	2215:00
ROFS21	29 Aug. 2001	1011:00
ROFS22	01 Sept. 2001	1035:00
ROFS23	05 Sept. 2001	2005:00
ROFS24	06 Sept. 2001	0943:00
ROFS25	08 Sept. 2001	1024:00
ROFS26	11 Sept. 2001	0922:00
ROFS27	11 Sept. 2001	0951:00
ROFS28	14 Sept. 2001	0916:00
ROFS29	14 Sept. 2001	1016:00
ROCH30	14 Sept. 2001	1044:00

[a]The characters ''FS'' in the flight label indicates a falling sphere, a ''CH'' a foil cloud (chaff). Flight ROFS26 was a failure.

[6] Several ground-based instruments performed measurements in the upper atmosphere during ROMA. The most important data in this context are the temperatures obtained by the potassium lidar of the Leibniz-Institute of Atmospheric Physics in Kühlungsborn [*von Zahn and Höffner*, 1996]. This technique deduces atmospheric temperatures in the potassium layer from measurements of the spectral width of the Doppler broadened absorption line of K atoms. The lidar was brought to Svalbard in May 2001 and gave temperature profiles between approximately 85 and 100 km, most of them were taken during full daylight conditions. A detailed presentation of data from this lidar will be given in a future publication. The lidar temperatures are available at 15 min and 1 km interval. To obtain the start temperature mentioned above these profiles have been averaged over 24 hours and a running mean over the summer season was calculated. The uncertainty of the K lidar temperatures is typically a few Kelvin. The availability of the K lidar temperatures significantly improves the FS data analysis since the uncertainty in start temperature T_o described in the previous section, is reduced substantially.

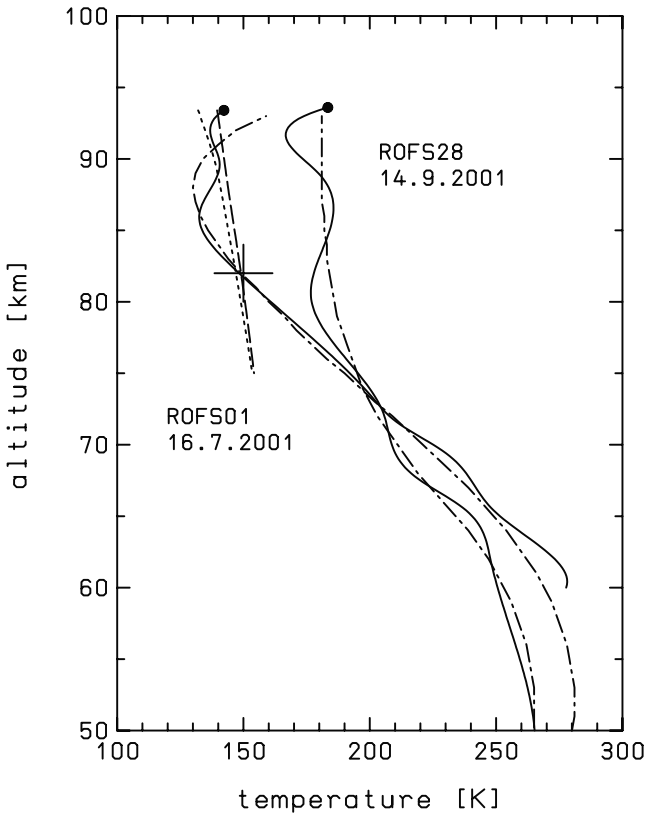

Figure 1. Temperature profiles from flights ROFS01 and ROFS28 measured on 16 July and 14 September 2001, respectively (solid lines). The dashed-dotted lines show the corresponding mean profiles from 69°N from the study of *Lübken* [1999] for the months 7.5 and 9.5, respectively (nomenclature from Table 2). The short-dashed line indicates frost point temperatures T_f using model water vapor mixing ratios from the study of *Körner and Sonnemann* [2001]. The long-dashed line shows T_f using a water vapor mixing ratio of 5 ppmv independent of altitude.

[7] Another ground-based instrument of importance here is the SOUSY (sounding system) VHF radar of the Max-Planck Institute for Aeronomie Katlenburg-Lindau (Germany) which is installed only 15 km from the launch site [*Czechowsky et al.*, 1998]. A detailed comparison of PMSE detected by this radar with temperature profiles reported here will be presented in the future.

[8] In Figure 1, two temperature profiles are shown: One is the very first measured in the mesosphere at these high latitudes (ROFS01 on 16 July), and the other is a typical profile from the end of the campaign (ROFS28 from 14 September). For comparison we show mean profiles from a compilation of measurements at Andøya (69°N, 16°E), i.e., at a similar longitude but approximately 10° further south [*Lübken*, 1999]. This compilation will hereafter be referred to as "FJL-JGR99." The ROFS01 temperature profile in Figure 1 shows a double structured mesopause region with minimum temperatures of 137 and 133 K at 93 and 86 km, respectively. The latter is close to the minimum temperature at 69°N (=130 K). Compared to ROFS01 the temperatures from flight ROFS28 measured on 14 September are much higher by up to 30–50 K in the upper mesosphere. Furthermore, in the lower mesosphere July temperatures are higher compared to September. This is presumably due to stronger heating by absorption of solar UV radiation by the Hartley bands of ozone.

[9] In Figure 2, the temperature profiles are grouped according to season. Flights ROFS01-ROFS17 (16 July to 23 August) are typical for the main summer season with very little variability from flight to flight (Figure 2a). The remaining flights are from the transition period between summer and winter. The first flights in this period are ROFS18-ROFS22 (27 August to 1 September) and are shown as dotted lines in Figure 2b. The remaining profiles, namely from flights ROFS23-ROFS29 (5–14 September) are shown as solid lines in Figure 2b together with the climatological mean from FJL-JGR99 for the beginning of September. The temperatures are much higher compared to summer and are also somewhat more variable from flight to flight. Furthermore, a mesopause cannot clearly be identified which indicates that the minimum temperature is located above the upper altitude limit of the FS technique.

[10] In order to obtain a seasonal variation of temperatures we have taken all measurements at a given altitude and calculated the mean temperature in time bins of 0.25 months. These mean temperatures were then smoothed by spline fitting. This procedure was repeated at all altitudes from 55 up to 92 km. From the spline fits, we have evaluated temperature profiles as a function of altitude at time intervals of ~1 week. These T(z) profiles were again slightly smoothed in order to remove minor "wiggles" in the profiles. The RMS deviation of the individual measurements from the smoothed temperature field is typically 3–5 K in the upper mesosphere. The variability increases around the mesopause. The smoothed temperature profiles are shown as a function of season in Figure 3 and are listed in Table 2. Note the very cold summer mesopause at ~89–90 km with temperatures below 130 K and the transition from summer to winter at the end of August.

[11] It is interesting to note that at mesopause altitudes the temperature actually decreases slightly in the first 1–2 weeks of the campaign (see Figure 3). For example, at 88 km the temperature decreases by 4 K from mid-July to beginning of August (see Table 2). We have carefully checked that this decrease is not caused by the local temperature maximum observed in the very first flight (see Figure 1) by approximating the ROFS01 profile by a smooth profile which no longer shows the local maximum. The small temperature decrease is in fact present in the first 5 flights and therefore shows up in the smoothed mean profiles of Table 2. Whether or not this decrease is of geophysical relevance cannot definitely be stated here since the number of measurements is comparatively small.

[12] The individual mass density profiles were smoothed similarly to the temperatures, i.e., the raw densities at a given altitude were averaged and a spline fit was determined to the logarithm of the average densities. Flights ROFS06 and ROFS09 were ignored in this procedure since there was an apparent offset in the densities probably caused by a partial collapse of the sphere (the temperatures rely on the density gradients that were apparently not

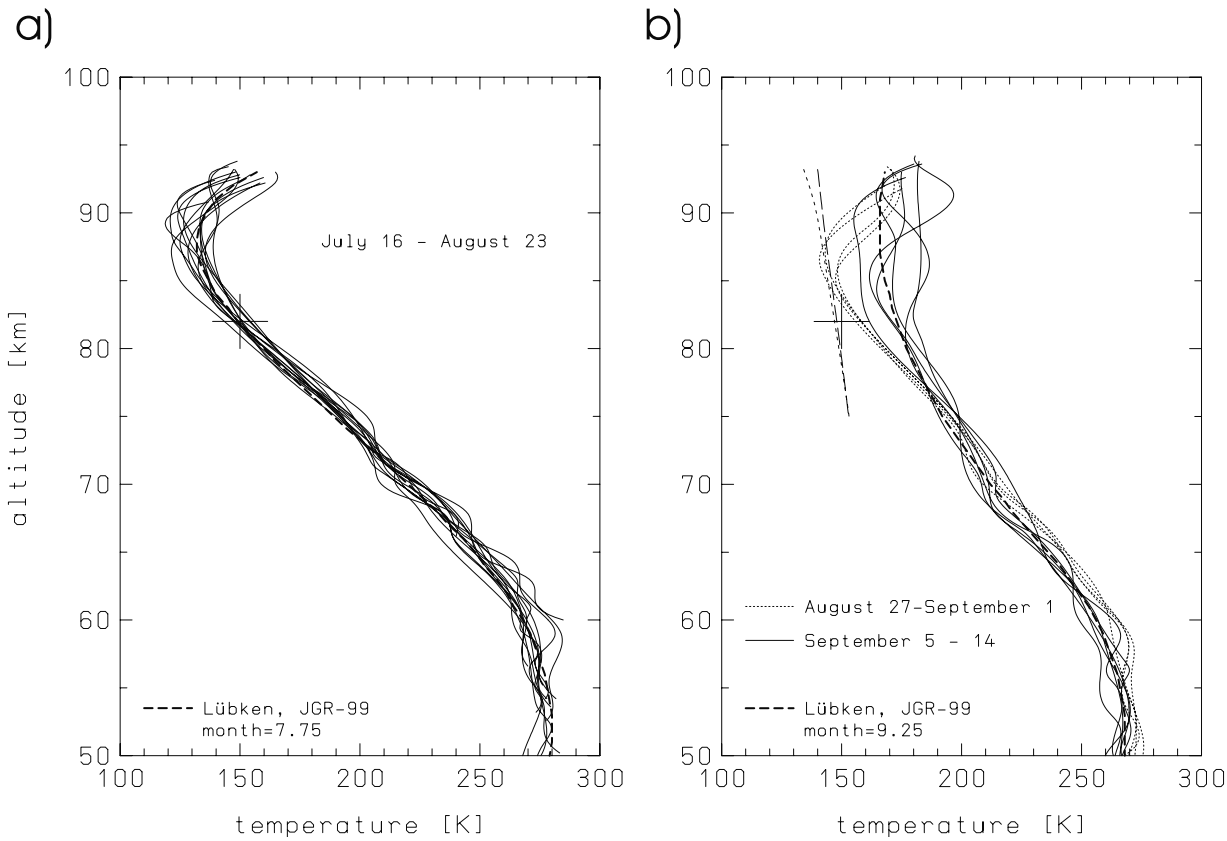

Figure 2. (a) All temperature profiles measured during the summer season, more precisely from 16 July to 23 August. For comparison, T = 150°K at 82 km is marked by a cross and the mean temperature profile from 69°N for month 7.75 (nomenclature from Table 2) from the study of *Lübken* [1999] is shown. (b) All temperature profiles measured from 5 to 14 September (solid lines) and in the interim period (dotted line). The mean profile from FJL-JGR99 is shown for month 9.25. The short-dashed line indicates frost point temperatures T_f using model water vapor mixing ratios from the study of *Körner and Sonnemann* [2001]. The long-dashed line shows T_f using a water vapor mixing ratio of 5 ppmv independent of altitude.

affected). The densities resulting from this procedure are listed in Table 3.

3. Discussion

3.1. Temperatures in the Mesopause Region

[13] We start the discussion of our temperature measurements by presenting all individual data points at an altitude of 82 km, i.e., at typical NLC altitudes in Figure 4 [*Lübken et al.*, 1996; *Fiedler et al.*, 2003]. Until approximately the end of August (more precisely 23 August) the temperatures are very close to 150 K. The mean of these temperatures is 150.0 K with an RMS deviation of ±3.0 K and a maximum deviation of +5.6 and −6.4 K from the mean (individual temperatures at 82 km are listed in Table 4). A temperature of 150 K at 82 km has frequently been observed in the summer season at 69°N, and even at Antarctic latitudes (68°S) [*Lübken*, 1999; *Lübken et al.*, 1999]. This surprising steadiness of the thermal structure at NLC/PMSE altitudes has earlier been labeled "equithermal submesopause."

[14] In Figure 4, the transition from summer to winter occurs after approximately the end of August which is significantly later compared to 69°N. This implies that at 82 km the atmosphere is significantly colder by ∼5–10 K compared to FJL-JGR99 from mid-August to the end of the ROMA campaign. We note, however, that the database leading to the FJL-JGR99 climatology is rather limited in the transition period and that this difference could at least partly be due to natural variability.

[15] For each profile in the summer season (16 July to 23 August), we have derived the mesopause altitude and temperature (see Table 4). The mean mesopause temperature is 128 ± 6 K at an altitude of 89 ± 1.5 km, where the variability given is the RMS deviation from the mean. A closer look to the smoothed temperatures in Table 2 shows that the mesopause temperature actually decreases from 130 K in mid-July to 126–128 K until the first week in August, whereas the mesopause altitude is approximately constant in this period. The double layered mesopause observed in flight ROFS01 (see Figure 1) is not a prominent feature in our measurements. We see a clear double structured mesopause in only two flights (ROFS01 and ROFS07) and a weak tendency to such a structure in two more flights (ROFS02 and ROFS03), i.e., in only 2(+2) out of 14 flights in the summer season. We note that a double structured mesopause has occasionally been observed at 69°N. This

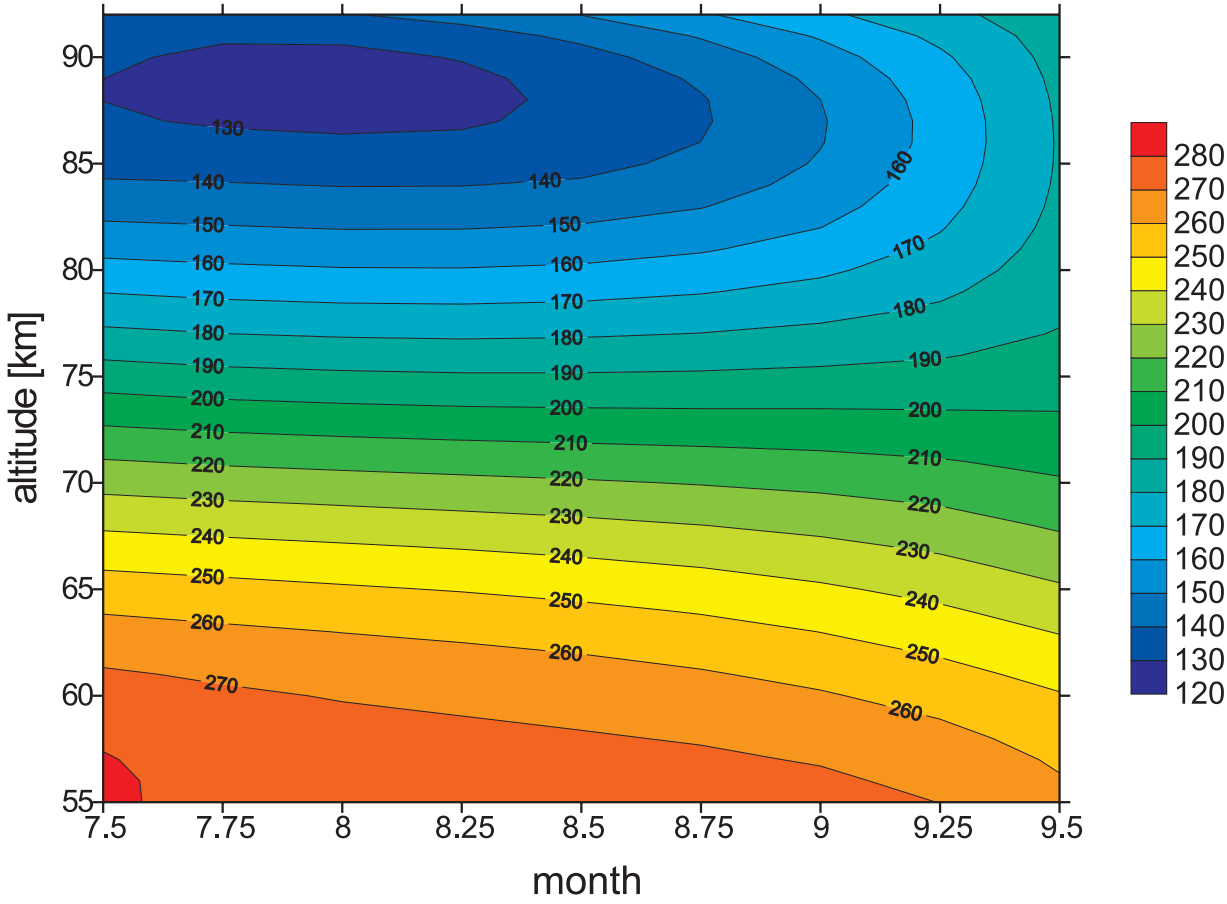

Figure 3. Contour plot of the seasonal variation of mean falling sphere temperatures from 16 July to 14 September at 78°N. Individual measurements have been averaged and smoothed (see text for more details). Temperatures are listed in Table 2. The color code is explained in the insert (values in K).

feature should not be mixed with the double mesopause structure described by *Berger and von Zahn* [1999], which is a persistent and not a sporadic feature with temperature minima at 88 and 100 km, respectively. The upper minimum is above the height range of the FS technique.

3.2. Comparison With Data From 69°N and With the IAP Version of the Cologne Model of the Middle Atmosphere (COMMA/IAP) Model

[16] A comparison of our data with other measurements at the same or at similar latitudes is not possible since no temperature data exist for the major part of the mesosphere. There have been several Russian rocket sonde launches from Heiss Island (81°N) but this technique gives reliable temperatures only below ~65 km. We therefore concentrate on a comparison with similar measurements at 69°N (Andøya) summarized in FJL-JGR99.

[17] A systematic comparison of the ROMA results with the temperature climatology of FJL-JGR99 shows that the thermal structure is basically similar, i.e., it shows a very cold mesosphere and little variability of the temperature profiles in the mesosphere during summer (compare Figure 2a with Figure 7 in FJL-JGR99). However, there are also some systematic differences: In the upper mesosphere at 85–90 km temperatures are lower at 78°N compared to 69°N by ~5–7 K from late July to beginning of September. In the lower mesosphere at 63–73 km, temperatures are higher at 78°N compared to 69°N by ~5 K from mid-July (the beginning of the ROMA campaign) to mid-August. It should be pointed out that the FJL-JGR99 climatology in midsummer is based on several years of measurements, whereas data from one year only are available at Spitsbergen. This means that we cannot account for any year-to-year variability in our comparison.

[18] We have compared the mesopause altitude and temperature for the main summer season part of ROMA using the mean smoothed temperatures presented in Table 2 and similar data presented in FJL-JGR99. In the time period 7.50–8.25 (nomenclature from Table 2) the mean difference of mesopause heights is approximately +0.9 km (higher at Longyearbyen compared to Andøya). We note that this difference is marginal taking into account the height resolution of the FS technique. The mesopause temperature difference is negligible in mid-July but temperatures are approximately 6–8 K lower at Longyearbyen compared to Andøya in the second half of July and in August. Part of this difference (especially in late August) is due to the later transition from summer to winter in Longyearbyen. We summarize that in the summer season the mesopause at 78°N is somewhat higher (by ~1 km) and, at the end of the summer season, somewhat colder (by ~5–6 K) compared to 69°N.

Table 2. Seasonal Variation of FS Temperatures at 78°N[a]

z	Month of the Year								
(km)	7.50	7.75	8.00	8.25	8.50	8.75	9.00	9.25	9.50
55	282	276	273	273	273	274	273	270	262
56	282	276	274	273	273	273	271	268	261
57	281	276	274	273	272	271	269	265	259
58	279	275	273	272	271	269	267	263	257
59	277	274	272	270	269	267	264	260	254
60	274	271	269	268	266	264	261	256	251
61	271	269	267	265	263	261	258	253	247
62	268	265	264	262	260	257	254	249	243
63	264	262	260	258	256	253	250	245	240
64	259	257	256	254	252	249	246	241	235
65	255	253	251	249	247	245	241	237	231
66	250	248	246	245	243	240	237	233	227
67	244	243	241	239	238	235	232	229	223
68	239	237	235	234	232	230	228	224	219
69	233	231	230	228	227	225	223	220	215
70	227	225	224	222	221	219	218	215	211
71	221	219	217	216	215	214	213	211	208
72	214	212	211	210	209	208	208	206	204
73	208	206	205	204	203	203	202	202	201
74	202	200	198	197	197	197	197	198	198
75	195	193	192	191	191	191	192	193	195
76	189	187	185	185	185	186	187	189	193
77	182	180	179	179	179	180	182	185	191
78	176	174	173	172	173	175	178	182	189
79	170	168	167	166	167	169	173	178	187
80	163	162	161	161	162	164	168	175	185
81	157	156	155	155	156	159	164	172	184
82	152	151	150	150	151	154	160	169	183
83	146	145	144	145	146	150	156	167	182
84	141	141	140	140	141	146	153	165	181
85	137	136	135	135	137	142	151	164	181
86	134	132	131	132	134	140	150	163	181
87	131	129	128	129	132	139	149	163	181
88	130	127	126	128	132	139	150	164	181
89	130	126	126	128	133	141	152	166	182
90	132	128	127	131	137	145	156	168	183
91	135	131	132	136	142	151	161	172	185
92	140	138	139	144	150	159	168	177	186

[a]Temperatures in K. Month of the year: 8.0, August 1; 8.5, August 15; etc.

Table 3. Seasonal Variation of FS Mass Densities at 78°N[a]

z	Month of the Year								
(km)	7.50	7.75	8.00	8.25	8.50	8.75	9.00	9.25	9.50
55	3.16	3.16	3.16	3.18	3.20	3.22	3.25	3.26	3.29
56	3.21	3.21	3.22	3.23	3.25	3.27	3.30	3.32	3.34
57	3.26	3.26	3.27	3.29	3.30	3.33	3.35	3.37	3.39
58	3.31	3.31	3.32	3.34	3.36	3.38	3.40	3.42	3.44
59	3.36	3.36	3.37	3.39	3.41	3.43	3.45	3.47	3.49
60	3.41	3.41	3.42	3.44	3.46	3.48	3.50	3.52	3.54
61	3.46	3.46	3.47	3.49	3.51	3.53	3.55	3.57	3.60
62	3.50	3.51	3.52	3.54	3.56	3.58	3.60	3.63	3.65
63	3.55	3.56	3.57	3.59	3.61	3.63	3.65	3.68	3.70
64	3.60	3.61	3.62	3.64	3.66	3.68	3.70	3.73	3.76
65	3.65	3.66	3.67	3.69	3.71	3.73	3.75	3.78	3.82
66	3.70	3.71	3.72	3.74	3.76	3.78	3.81	3.84	3.87
67	3.75	3.76	3.77	3.79	3.81	3.83	3.86	3.89	3.93
68	3.80	3.81	3.82	3.84	3.86	3.89	3.91	3.95	3.99
69	3.85	3.86	3.87	3.89	3.91	3.94	3.97	4.00	4.05
70	3.90	3.91	3.93	3.94	3.97	3.99	4.03	4.06	4.11
71	3.95	3.96	3.98	4.00	4.02	4.05	4.08	4.12	4.17
72	4.01	4.02	4.03	4.05	4.08	4.11	4.14	4.18	4.23
73	4.07	4.08	4.09	4.11	4.14	4.17	4.20	4.25	4.29
74	4.12	4.13	4.15	4.17	4.20	4.23	4.27	4.31	4.36
75	4.18	4.19	4.21	4.23	4.26	4.29	4.33	4.37	4.43
76	4.24	4.25	4.27	4.29	4.32	4.35	4.39	4.44	4.49
77	4.31	4.32	4.34	4.36	4.39	4.42	4.46	4.51	4.56
78	4.37	4.39	4.40	4.43	4.45	4.49	4.53	4.58	4.64
79	4.44	4.45	4.47	4.50	4.52	4.56	4.60	4.65	4.71
80	4.51	4.53	4.55	4.57	4.60	4.63	4.67	4.73	4.78
81	4.59	4.60	4.62	4.65	4.67	4.71	4.75	4.80	4.86
82	4.66	4.68	4.70	4.73	4.75	4.79	4.83	4.88	4.94
83	4.75	4.76	4.79	4.81	4.84	4.87	4.91	4.96	5.02
84	4.83	4.85	4.87	4.90	4.92	4.96	5.00	5.04	5.10
85	4.92	4.94	4.96	4.99	5.02	5.05	5.09	5.13	5.18
86	5.02	5.04	5.06	5.08	5.11	5.14	5.18	5.21	5.26
87	5.12	5.14	5.16	5.18	5.21	5.24	5.27	5.30	5.34
88	5.22	5.24	5.26	5.29	5.32	5.35	5.37	5.39	5.42
89	5.33	5.35	5.37	5.40	5.43	5.45	5.48	5.49	5.49
90	5.45	5.46	5.49	5.52	5.54	5.57	5.58	5.58	5.57
91	5.57	5.58	5.61	5.64	5.67	5.69	5.70	5.68	5.64
92	5.70	5.71	5.73	5.76	5.79	5.81	5.81	5.78	5.71

[a]Read, e.g., "3.57" as $10^{-3.57}$ kg/m^3. Month of the year: 8.0, 1 August; 8.5, 15 August, etc.

[19] It is interesting to note that the variation of the summer mesopause altitude and temperature with latitude is also present in the IAP version of the Cologne Model of the Middle Atmosphere (COMMA/IAP) [*Berger and von Zahn*, 1999; *von Zahn and Berger*, 2003]. For midsummer conditions, this model predicts a mesopause altitude increase by approximately 1 km per 10° latitude and a corresponding mesopause temperature decrease by approximately 8–10 K, in general agreement with our observations.

[20] The mass densities at both sites are very similar in the entire mesosphere for the months of overlapping data (deviations less than 6%), except in the upper mesosphere (above approximately 78 km) from mid-July to mid-August, where densities at 78°N are higher by up to 12% relative to 69°N.

[21] It is obvious from Figure 4 that our temperature measurements are significantly lower compared to the COSPAR International Reference Atmosphere (CIRA, 1986) and also lower, but to a lesser extent, compared to the MSIS (mass spectrometer and incoherent scatter data) empirical model [*Fleming et al.*, 1990; *Hedin*, 1991]. In the upper mesosphere from mid-July to beginning of Septem-

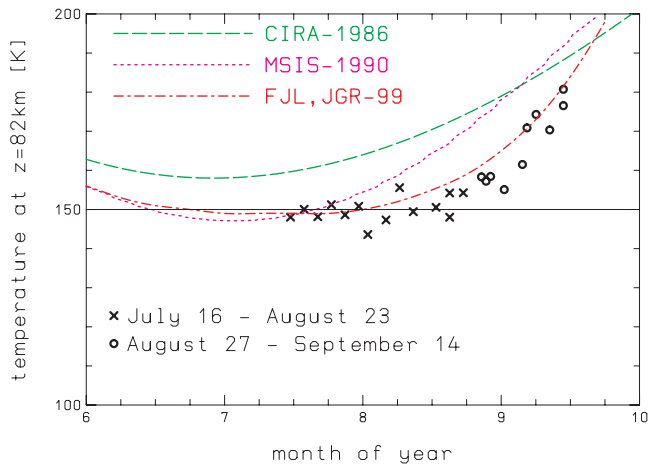

Figure 4. Falling sphere temperatures at an altitude of 82 km as a function of season. Data from the summer period are marked by crosses and the remaining measurements by circles. For comparison, we show two reference profiles, namely CIRA (1986) (long-dashed line) and MSIS-1990 (short-dashed line), and the climatology from 69°N [*Lübken*, 1999].

Table 4. Temperatures at 82 km and at the Mesopause for the Summer Flights in ROMA[a]

Flight Label	Date	T(82 km)	z_M	T_M
ROFS01	16 July	148.0	86.2	132.1
ROFS02	19 July	150.0	91.0	123.4
ROFS03	22 July	148.1	88.8	118.6
ROFS05	25 July	151.2	87.6	124.5
ROFS06	28 July	148.6	89.6	120.0
ROFS07	31 July	150.8	92.0	137.5
ROFS09	02 Aug.	143.6	87.4	120.5
ROFS10	06 Aug.	147.3	89.6	123.8
ROFS11	09 Aug.	155.6	89.0	126.5
ROFS12	12 Aug.	149.4	89.4	132.5
ROFS13	17 Aug.	150.6	89.0	134.0
ROFS15	20 Aug.	148.0	87.2	127.4
ROFS16	20 Aug.	154.2	88.6	133.1
ROFS17	23 Aug.	154.3	87.0	135.0

[a]T(82 km) is the temperature at an altitude of 82 km (in K). z_M and T_M are the mesopause heights (in km) and temperatures (in K), respectively. The mean mesopause temperature and height are 127.8 K and 88.7 km, respectively, with a RMS variability of 6.0 K and 1.5 km.

ber, the difference to CIRA (1986) is typically −10 to −20 K and the difference to MSIS is 0 to −18 K.

3.3. Implications for the Existence of Ice Particles

[22] We will now discuss in more detail the relationship between the seasonal variation of upper mesospheric temperatures and the occurrence rate of PMSEs and NLCs. The existence of these layers is critically determined by the degree of saturation $S = p_{H_2O}/p_{sat}$, where p_{H_2O} is the partial pressure of water vapor and p_{sat} is the saturation pressure of water vapor over ice as given by *Marti and Mauersberger* [1993]:

$$\log_{10} p_{sat} = 12.537 - (2663.5/T) \quad (1)$$

where p_{sat} is in N/m^2 and T is in K. If $S > 1$, the particles can exist or grow, and if $S < 1$, they will evaporate. The frost point temperature T_f is obtained by solving (1) for temperature using $S = 1$. The water vapor mixing ratios $[H_2O]$ required to determine p_{H_2O} and T_f were taken from the theoretical model of *Körner and Sonnemann* [2001]. Typical mixing ratios in July vary from 4.1 to 0.5 ppmv at 75 and 93 km, respectively. In the upper mesosphere, $[H_2O]$ increases slightly by ~1 ppmv from July to August. We note that these are mean water vapor mixing ratios which do not take into account freeze drying effects etc. [e.g., *von Zahn and Berger*, 2003].

[23] In Figure 1, we show the frost point temperatures T_f using $[H_2O]$ from the study of *Körner and Sonnemann* [2001]. We also show T_f for a constant mixing ratio of 5 ppmv, which demonstrates that $[H_2O]$ does not critically determine the height range of supersaturation. In an extended altitude range between approximately 82 and 92 km the actual temperatures are lower than T_f indicating that it is cold enough at these heights for ice particles to grow or exist. Indeed, a PMSE was observed during the ROFS01 flight at exactly this altitude range (Röttger, private communication, 2002). During summer, all temperature profiles showed an altitude range of several km in the upper mesosphere with supersaturation (see Figure 2a). For example, at 87 km the frost point temperature is $T_f = 143$ K which is larger than the maximum temperature observed at this height ($T_{max} = 138$ K). It is obvious from Figure 1 that the actual temperatures from ROFS28 are much higher compared to T_f so that ice particles cannot exist. In the transition period (ROFS18-ROFS22 in Figure 2b) temperatures can still be very low, say below 150 K, but are only marginally below T_f. The altitude range where ice particles can exist is rather small (a few km only). The profile from ROFS22 on 1 September is the last in our sequence where temperatures were close to T_f.

[24] In Figure 5, we show a contour plot of the degree of saturation as a function of altitude and season based on the temperatures and densities presented in Tables 2 and 3, respectively, and the model water vapor values from the study of *Körner and Sonnemann* [2001]. As can be seen from Figure 5, ice particles can exist or grow in an altitude range from approximately 82 to 92 km in midsummer. Large supersaturation values of $S > 40$ occur around the summer mesopause and even larger values of $S > 100$ are derived. The altitude range for $S > 1$ shrinks with progressing season and disappears at the end of August. The slight decrease of temperatures in the upper mesosphere at the beginning of the campaign (discussed in section 2) results in an even more prominent change of S.

[25] Very little information is available regarding the occurrence frequency of NLC, PMSE, and PMC at very high latitudes. In a recent publication by *Rüster et al.* [2001], first results obtained with the SOUSY radar on Svalbard are presented. During the main summer season, PMSEs are frequently detected at altitudes between 82 and 92 km, consistent with our temperature measurements. We note, however, that the double layered structure observed in PMSEs are most likely not caused by the thermal structure since double layered mesopause temperatures are not a prominent feature in our observations (see above). This is probably not surprising since the occurrence of low enough temperatures (more precisely the existence of ice particles) is a necessary but not sufficient condition for PMSE [*Cho and Röttger*, 1997; *Lübken et al.*, 2002; *Rapp et al.*, 2003]. Furthermore, there could be temperature variations present

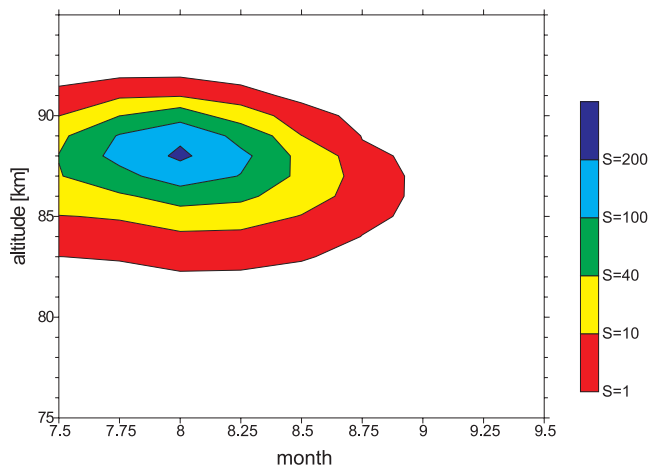

Figure 5. Degree of saturation using the temperature and density measurements listed in Tables 2 and 3, respectively, and water vapor concentrations from the model of *Körner and Sonnemann* [2001]. The color code is explained in the insert.

which are smaller than the altitude resolution of the FS technique and require more sophisticated in situ techniques [*Rapp et al.*, 2001]. Model calculations can probably help to clarify the relationship between PMSE and the thermal structure at these latitudes.

4. Summary

[26] In summary, we have performed the first in situ measurements covering the altitude range of the entire mesosphere at very high latitudes (78°N) in the ROMA campaign in 2001. A total of 24 temperature profiles were measured from 16 July to 14 September from Longyearbyen on Svalbard. During the summer period (16 July to mid-August) the mean mesopause temperature and altitude is 128 K and 89 km with a RMS variability of ±6 K and ±1.5 km, respectively. The mesopause temperature actually decreases slightly from ~130 K in mid-July to 126–128 K in late July and beginning of August. Compared to 10° further south (69°N, Andøya) the mesopause temperature is very similar in mid-July but significantly lower by 6–8 K in the second half of July and in August. Part of this difference (especially in late August) is due to the later transition from summer to winter in Longyearbyen. The mesopause altitude is higher by approximately 1 km at Longyearbyen compared to Andøya. The summer season in the upper mesosphere lasts until the third week in August, which is longer compared to lower latitudes. At 82 km, the temperature in summer is very close to 150 K, which is very similar to 69°N and to 68°S (''equithermal submesopause''). This surprising steadiness of the thermal structure at NLC/PMSE altitudes implies a major constraint on model calculations. In the upper mesosphere mean temperatures derived from our individual flights are significantly lower compared to CIRA (1986) (by up to 20 K) and also lower compared to MSIS.

[27] Assuming water vapor concentrations from a model we find supersaturation in an altitude range from approximately 82 to 92 km until mid-August. Using smoothed temperature and density fields we occasionally derive very large degrees of saturation (larger than 100) around the mesopause. The last flight where a height region with supersaturation was derived took place on 1 September.

[28] Our temperature measurements are in general agreement with the occurrence morphology of PMSE. However, within the altitude resolution of the FS technique double layered structures frequently observed in PMSEs are not a prominent feature of the thermal structure in the upper summer mesosphere. Model simulations will probably help to better understand the relationship between layered structures at high latitudes (NLC, PMSE, and PMC) and the thermal structure in the upper mesosphere.

[29] **Acknowledgments.** The excellent work by the crew of the Mobile Raketenbasis (DLR, Germany) and the Andøya Rocket Range is gratefully acknowledged. We thank Josef Höffner for providing potassium lidar temperatures. This project was supported by the Bundesministerium für Bildung, Wissenschaft, Forschung und Technologie, Bonn, under grant 50 OE 99 01.

References

Akmaev, R. A., Simulation of large-scale dynamics in the mesosphere and lower thermosphere with the Doppler-spread parameterization of gravity waves, 2, Eddy mixing and the diurnal tide, *J. Geophys. Res.*, *106*, 1205–1213, 2001.

Berger, U., and U. von Zahn, The two-level structure of the mesopause: A model study, *J. Geophys. Res.*, *104*, 22,083–22,093, 1999.

Cho, J. Y. N., and J. Röttger, An updated review of polar mesosphere summer echoes: Observation, theory, and their relationship to noctilucent clouds and subvisible aerosols, *J. Geophys. Res.*, *102*, 2001–2020, 1997.

Czechowsky, P., J. Klostermeyer, J. Röttger, R. Rüster, and G. Schmidt, The Sousy-Svalbard-Radar for middle and lower atmosphere research in the polar region, in *Proc. of the 8th Workshop on Tech., Sci. Aspects of MST Radar*, edited by B. Edwards, pp. 318–321, SCOSTEP, Boulder, Colo., 1998.

Fiedler, F., G. Baumgarten, and G. von Cossart, Noctilucent clouds above ALOMAR between 1997 and 2001: Occurrence and properties, *J. Geophys. Res.*, *108*, doi:10.1029/2002JD002419, in press, 2003.

Fleming, E. L., S. Chandra, J. J. Barnett, and M. Corney, Zonal mean temperature, pressure, zonal wind, and geopotential height as functions of latitude, *Adv. Space Res.*, *10*(12), 11–59, 1990.

Forbes, J. M., Atmospheric tides, 2, The solar and lunar semidiurnal components, *J. Geophys. Res.*, *87*, 5241–5252, 1982.

Garcia, R. R., and S. Solomon, The effect of breaking gravity waves on the dynamics and chemical composition of the mesosphere and lower thermosphere, *J. Geophys. Res.*, *90*, 3850–3868, 1985.

Hedin, A. E., Extension of the MSIS thermosphere model into the middle and lower atmosphere, *J. Geophys. Res.*, *96*, 1159–1172, 1991.

Körner, U., and G. R. Sonnemann, Global 3D-modeling of the water vapor concentration of the mesosphere/mesopause region and implications with respect to the NLC region, *J. Geophys. Res.*, *106*, 9639–9651, 2001.

Lübken, F. J., Thermal structure of the Arctic summer mesosphere, *J. Geophys. Res.*, *104*, 9135–9149, 1999.

Lübken, F. J., et al., Intercomparison of density and temperature profiles obtained by lidar, ionization gauges, falling spheres, datasondes, and radiosondes during the DYANA campaign, *J. Atmos. Terr. Phys.*, *56*, 1969–1984, 1994.

Lübken, F. J., K.-H. Fricke, and M. Langer, Noctilucent clouds and the thermal structure near the Arctic mesopause, *J. Geophys. Res.*, *101*, 9489–9508, 1996.

Lübken, F. J., M. J. Jarvis, and G. O. L. Jones, First in situ temperature measurements at the Antarctic summer mesopause, *Geophys. Res. Lett.*, *26*, 3581–3584, 1999.

Lübken, F. J., M. Rapp, and P. Hoffmann, Neutral air turbulence and temperatures in the vicinity of polar mesosphere summer echoes, *J. Geophys. Res.*, *107*(D15), 4273, doi:10.1029/2001JD000915, 2002.

Marti, J., and K. Mauersberger, A survey and new measurements of ice vapor pressure at temperatures between 170 and 250 K, *Geophys. Res. Lett.*, *20*, 363–366, 1993.

Rapp, M., J. Gumbel, and F. J. Lübken, Absolute density measurements in the middle atmosphere, *Ann. Geophys.*, *19*, 571–580, 2001.

Rapp, M., F.-J. Lübken, A. Müllemann, G. E. Thomas, and E. J. Jensen, Small scale temperature variations in the vicinity of NLC: Experimental and model results, *J. Geophys. Res.*, *107*(D19), 4392, doi:10.1029/2001JD001241, 2002.

Rapp, M., F.-J. Lübken, P. Hoffmann, R. Latteck, G. Baumgarten, and T. Blix, PMSE dependence on aerosol charge number density and aerosol size, *J. Geophys. Res.*, *108*(D8), 8441, doi:10.1029/2002JD002650, 2003.

Rüster, R., J. Röttger, G. Schmidt, P. Czechowsky, and J. Klostermeyer, Observations of mesospheric summer echoes at VHF in the polar cap region, *Geophys. Res. Lett.*, *28*, 1471–1474, 2001.

Schmidlin, F. J., The inflatable sphere: A technique for the accurate measurement of middle atmosphere temperatures, *J. Geophys. Res.*, *96*, 22,673–22,682, 1991.

von Zahn, U., and U. Berger, Freeze-drying at the summer polar mesopause: Its likely persistence and consequences, *J. Geophys. Res.*, *108*, doi:10.1029/2002JD002409, in press, 2003.

von Zahn, U., and J. Höffner, Mesopause temperature profiling by potassium lidar, *Geophys. Res. Lett.*, *23*, 141–144, 1996.

Widdel, H. U., Foil chaff clouds as a tool for in-situ measurements of atmospheric motions in the middle atmosphere: Their flight behaviour and implications for radar tracking, *J. Atmos. Terr. Phys.*, *52*, 89–101, 1990.

Zhu, X., J.-H. Yee, and E. R. Talaat, Diagnosis and dynamics and energy balance in the mesosphere and lower thermosphere, *J. Atmos. Sci.*, *58*, 2441–2454, 2001.

F.-J. Lübken and A. Müllemann, Leibniz-Institute of Atmospheric Physics, Schloss-Str. 6, D-18225, Kühlungsborn, Germany. (luebken@iap-kborn.de)